Journal of Applied Polymer Science

Poly(butylene succinate)/Layered Double Hydroxide Bionanocomposites: Relationships between Chemical Structure of LDH Anion, Delamination Strategy, and Final Properties

Laura Sisti,[1] Grazia Totaro,[1] Maurizio Fiorini,[1] Annamaria Celli,[1] Christian Coelho,[2] Mohammed Hennous,[2] Vincent Verney,[2] Fabrice Leroux[2]

[1]Dipartimento di Ingegneria Civile, Chimica, Ambientale e dei Materiali, Università di Bologna, Via Terracini 28, 40131 Bologna, Italy

[2]Institut de Chimie de Clermont Ferrand (ICCF)-UMR 6296 Université Blaise Pascal, 24 Avenue des Landais, 63177 AUBIERE (cedex), France

Correspondence to: L. Sisti (E-mail: laura.sisti@unibo.it)

ABSTRACT: A series of poly(butylene succinate) (PBS) containing organo-modified layered double hydroxide (LDH) are prepared by melt compounding and by *in situ* polymerization of succinic ester and 1,4-butanediol. Various LDHs intercalated with renewable organic anions are used. More specifically, lauryl sulfate, stearate, succinate, adipate, sebacate, citrate, and ricinoleate ions are used as LDHs organo-modifiers. The thermal, rheological, and dynamic mechanical properties of the samples are investigated. The results reveal a general mechanical reinforcement imparted by the clays. Significant changes are observed for the *in situ* polymerized nanocomposites, especially for LDH stearate which improves the properties of PBS nanostructure, whereas very few differences are observed for the other samples. © 2013 Wiley Periodicals, Inc. J. Appl. Polym. Sci. 130: 1931–1940, 2013

KEYWORDS: biopolymers and renewable polymers; nanoparticles; nanowires and nanocrystals; properties and characterization

Received 7 January 2013; accepted 6 April 2013; Published online 10 May 2013
DOI: 10.1002/app.39387

INTRODUCTION

The development of biobased and biodegradable polymers aroused great interest in materials science for the protection of the environment.[1] Aliphatic polyesters represent a highly promising class of environment-friendly plastics. Among them, poly (butylene succinate) (PBS) is an interesting material with several good characteristics. It is synthesized starting from succinic acid and butanediol, both derivable from renewable resources.[2] Moreover, PBS is a commercially available semicrystalline thermoplastic, featuring biodegradability, melt processability, and thermal and chemical resistance, thus giving rise to a wide range of potential applications.[3] However, PBS presents some shortcomings, such as insufficient stiffness, low-melt strength and viscosity, low gas barrier properties. Hence, considerable efforts are now being focused on improving PBS properties in view of wider final applications.

Preparation of organic/inorganic nanocomposites is a very active area of research, as in general, very small amounts of filler lead to a significant enhancement of permeability and mechanical, thermal, electrical, and fire resistant properties, as compared to those of pure polymer or the conventional composites. Such enhanced properties are usually due to the small size of the structural unit, its large exposed surface area associated to adhesion between nanoparticles and the polymer that might result from attrition. As to nanofillers, such as silica,[4–6] titania,[7] carbon nanotubes,[8–10] graphene,[11] and so forth, layered plate-like particles have shown very promising results and achieved an adequate dispersion of the lamellar nanoparticles within the polymer matrix. Most work in this area was carried out on polymeric nanocomposites derived from layered phyllosilicates.[12–15] Hydrotalcite-like compounds, also known as layered double hydroxide (LDH) or anionic clays, are now gaining attention for this purpose, as they display specific advantages, such as purity, crystallinity, particle size control, tunable chemical composition in association to layer charge density, and easy functionalization as well as a marked biocompatibility because some LDH intralayer compositions are envisioned as reservoir for drug delivery[16] and gene reservoir[17] and more recently for nanoforensic by deciphering and undeciphering bar code by

Additional Supporting Information may be found in the online version of this article.

means of LDH-interleaved DNA molecules.[18] Non-miscible PBS LDH system using porphyrin as single oxygen-producing agent is also reported for photobiocide polymer activity.[19] In fact, the synthetic pathways to LDHs are very simple and inexpensive, allowing the production and use of products with a highly defined and reproducible composition.[20] Their crystalline structure consists of layers formed by octahedral units with shared edges. Each octahedron consists of M^{II} or M^{III} cations surrounded by six OH^-. The presence in the layer of M^{III} cations induces an excess positive charge balanced by exchangeable anions (A^{n-}) accommodated in the interlayer region where water molecules are also located. They could be represented by a general chemical formula $[M^{II}_{1-x}M^{III}_x(OH)_2]^{x+}A^{n-}_{x/n}\cdot mH_2O$.[21] The best known and naturally occurring anionic clay is hydrotalcite: $Mg_6Al_2(OH)_{16}CO_3\cdot 4H_2O$.

Currently, two main methods are used to prepare nanocomposites:[22] *in situ* polymerization in the presence of the clay and melt blending between polymer matrix and clay. The main feature of both methods is the so-called organo-modification of the inorganic layered materials.[11] In fact, what makes anionic and cationic clays suitable for nanocomposite preparation is the exchangeable or reactive nature of the interlayer guest molecule to endow the platelets with suitable organophilic character.

Generally, *in situ* polymerization involves reactions between nanoscale-modified additives and monomers, and the nanocomposites are formed during the bulk polymerization. The degree of dispersion of nanoparticles inside the polymeric matrix and the interfacial interaction are favorite and then advantages include easy handling and good performances of the final products.[23] A great disadvantage of this technique is the long processing time and this limits the application of *in situ* polymerization to industrial practice. On the other hand, a direct mixing of filler and polymer matrix by melt blending is little expensive, simple, fast, and compatible with current industrial techniques. The main difficulty in the mixing process is the effective dispersion of the fillers into the polymer matrix, because they usually tend to agglomerate.

In our knowledge, a directly comparison of these preparation method is not deeply tackled in literature. Hwang et al.[24] studied the effect of organoclay and preparation methods on the mechanical/thermal properties of polyamide-montmorillonite nanocomposites prepared by *in situ* polymerization and melt-compounding method; they found that samples have maximum tensile strength, wear resistance and cell density at montmorillonite loadings of 3 and 5 wt % for *in situ* polymerization and melt compounding, respectively.

Hernandez et al.[25] prepared transparent and conducting polymer nanocomposites based on poly(ethylene terephthalate) and single-wall carbon nanotubes (SWCNT) as additive, by direct mixing in the melt and by *in situ* polymerization, obtaining best performances in the first way. Moreover, they ascribed better electrical and optical properties of nanocomposites prepared by melt mixing in relation to those prepared by *in situ* process, to a certain level of aggregation of SWCNT, which favors the formation of electrical pathways and reduces the number of scatters of light, hence favoring the transmittance of the visible light through these materials.

Anyway, it is difficult to find in literature an indication on the best technique to prepare PBS/LDH nanocomposites. More numerous are the articles describing only one of these methodologies. It results that in general, exfoliated systems and, then, good final performances can be obtained by both methods, even if melt-blending procedure seems to show a poorer capability in inducing delamination in the nanocomposites.

Concerning melt blending, as example, Zhou et al.[26] studied the rheological properties of composites based on PBS and oleate/LDH prepared by melt compounding. They observe a tendency of the exfoliated system to form a gel-like rheological behavior, because of strong attrition phenomena. This is optimized for fillers loading as low as 3% w/w, while greater filler amount gives rise to platelet agglomeration without improvement of the rheological properties. Okamoto et al.[27] prepared PBS/organically modified layered silicate composites by melt extrusion, obtaining significantly rheological and dynamic mechanical properties improvement. Systems were both intercalated and exfoliated. Wei et al.,[28] for exfoliated PBS/LDH nanocomposites prepared by melt blending, found that crystallization rate is accelerated by the addition of fillers, due to its heterogeneous nucleation effect.

On the other hand, also *in situ* polymerization results to be an interesting approach to prepare well-dispersed systems. For example, Vassiliou et al.[5] prepared PBS/fumed silica nanocomposites by *in situ* polymerization and obtained interesting final properties. Finely dispersed SiO_2 nanoparticles into the PBS matrix were observed at low silica content, while some agglomerates formed at higher concentration. All tensile properties, except elongation at break, were significantly enhanced. Good dispersion and compatibility with polymer matrix, leading to enhanced mechanical properties, are reported also by Lim et al.[29] for similar nanocomposites based on PBS and fumed silica, prepared by *in situ* polymerization.

It is notable that a direct comparison between the final characteristics achieved in a specific nanocomposite prepared by following the two preparation techniques cannot be simply discussed, because the literature does not provide full data. For this reason, in this article, a directly comparison of the properties of the same nanocomposites, based on PBS and modified LDH obtained by these two different preparation procedures, is proposed, emphasizing a feature little explored in literature.

In particular, we describe the preparation of a class of bionanocomposites based on PBS and Mg-Al-based LDHs: *in situ* polymerization method starting from monomers and melt intercalation using a commercial PBS specimen. Clays are prepared with different organic anions as intercalating agents. In particular, sodium lauryl sulfate (LS), sodium stearate (ST), succinic acid, sebacic acid, adipic acid, citric acid (CA), and ricinoleic acid (RA) were used. Some of the organic species accommodated in the interlayers were chosen among organophilic fillers containing reactive functional groups. Indeed, if the organic intercalating agents feature at least one reactive

Table I. Organo-Modified LDH Synthesized

Code	Intercalating compound	Chemical composition[a]	Interlayer distance (Å)[b]
LDH-C	Sodium carbonate	$[Mg_{4.5}Al_2(OH)_{13}](C^{2-})_{1.0}2.7H_2O$	7.7
LDH-LS	Sodium lauryl sulfate	$[Mg_{4.5}Al_2(OH)_{13}](LS^{-})_{2.2}3.9H_2O$	34.4
LDH-ST_{Zn}	Sodium stearate	$[Mg_3Zn_1Al_2(OH)_{12}](ST^{-})_{1.2}2.9H_2O$	31.1
LDH-ST_{Mg}	Sodium stearate	$[Mg_{4.5}Al_2(OH)_{13}](ST^{-})_{2.4}1.5H_2O$	31.6
LDH-SU	Sodium succinate	$[Mg_{4.5}Al_2(OH)_{13}](SU^{2-})_{0.7}3.7H_2O$	10.9
LDH-AD	Sodium adipate	$[Mg_{4.5}Al_2(OH)_{13}](AD^{2-})_{0.8}4.1H_2O$	12.9
LDH-SE	Sodium sebacate	$[Mg_{4.5}Al_2(OH)_{13}](SE^{2-})_{0.7}4.6H_2O$	16.5
LDH-CA	Citric acid	$[Mg_6Al_3(OH)_{18}](CA^{3-})_{5.9}10.0H_2O$	12.0
LDH-RA	Ricinoleic acid	$[Mg_{4.5}Al_2(OH)_{13}](RA^{-})_{6.0}8.8H_2O$	30.3

[a] Anion and water content were determined by TGA.

[b] Determined by the first reflection in XRD analysis.

functional group that can react during the *in situ* intercalative polymerization, a stronger interaction between the polymer matrix and the nanoclay surface through its tethered molecules is expected leading to better mechanical properties. LDH modified with ST was also synthesized using Zn as divalent cation in addition to Mg: in fact, it is reported that the variation of the divalent metal cations in aluminum-containing LDHs may affects dispersion, thermal, and fire properties.[30,31] The novel clays and nanocomposites were fully characterized by different techniques, X-ray diffraction (XRD), thermal, rheological, and dynamic mechanical analyses which revealed that *in situ* polymerization together with a large-size organic molecule are the keys to yield a final material with improved mechanical properties.

EXPERIMENTAL

Materials

1,4-Butanediol (BD), dimethyl succinate (DMS), sodium carbonate (C), LS, ST, sodium succinate (SU), sodium sebacate (SE), sodium adipate (AD), CA, RA, sodium hydroxide, magnesium nitrate, aluminum nitrate, zinc nitrate, and dibutyl tin oxide were purchased from Aldrich Chemical. Commercial PBS (Natureplast PBE003) ($M_w = 84{,}000$) was obtained from Nature Plast. This sample will be indicated with the code PBE003 in the text. Another PBS sample was synthesized in our laboratory, following the procedure described in the *in situ* polymerization section, and will be indicated with the code PBSp. All the materials were used as received.

LDH Synthesis

In a typical procedure, 84 mmol of the organic anion (C, LS, ST, SU, AD, SE, or RA) are added in a 1-L three-necked, round-bottomed flask equipped with a reflux condenser, and a pH meter. Water or a solution of water/ethanol, in the case of ST and RA, was used to dissolve the salt. Once the salts were dissolved, the pH was raised to 10 with NaOH 2*M*. At this point, 11.5 g (45 mmol) of $Mg(NO_3)_2{\cdot}6H_2O$ and 7.5 g (20 mmol) of $Al(NO_3)_3{\cdot}9H_2O$, previously solubilized in 100 mL of water, were added dropwise, under nitrogen atmosphere, at room temperature, and under vigorous stirring, to the solution containing the organic anion. In the case of AD, LS, and ST, it was necessary to raise the temperature to 65–75°C in order for salt to remain dissolved. The pH was kept constant at 10 during the whole coprecipitation. The final mixture was left to react 16 h at 75–80°C, under vigorous stirring in nitrogen atmosphere. After that, the white solid was filtered, washed with 1 L of water or water and ethanol, and then dried at 100°C obtaining 6 g of finely ground powder characterized by XRD and FTIR analyses (data not shown). A second sample with ST was set starting from 12.4 g (40 mmol) of anion salt, 15.4 g (60 mmol) of $Mg(NO_3)_2{\cdot}6H_2O$, 15.0 g (40 mmol) of $Al(NO_3)_3 \cdot 9H_2O$, and 6.1 g (20 mmol) of $Zn(NO_3)_2{\cdot}6H_2O$: the procedure was the same described above. In the case of LDH prepared with CA, the method adopted was the one described by Zhang et al.[32] Citric acid (8.8 g, 42 mmol) was added to 100 mL of a water suspension of 4.0 g (8 mmol) of a previously prepared Mg/Al-LDH-carbonate, while temperature was kept at 50°C. The solution obtained was added dropwise to a NaOH solution (4.0 g, 0.10 mol) dissolved in 100 mL water keeping the pH above 9. The final mixture was left to react 2 h under reflux. The resulting solid was recovered as described previously for the other clays. The LDHs prepared are listed in Table I.

In Situ Polymerization

A round-bottomed, wide-neck glass reactor (250 mL capacity) was charged with the organo modified LDH (1.4 g, corresponding to 3 wt % with respect to the polymer theoretical yield), BD (30 g, 0.33 mol), and dibutyl tin oxide (0.30 g, 1.2×10^{-3} mol).

The reactor was closed with a three-necked flat flange lid equipped with a mechanical stirrer and a torque meter. The system was then connected to a water-cooled condenser and immersed in a thermostatic oil-bath at 200°C, while the stirrer was switched on at 100 rpm. After 1 h, the oil-bath was cooled to 180°C and DMS (40 g, 0.27 mol) was added to the reaction mixture; the temperature was then increased to 200°C and kept at this value until the entire methanol distilled off (~1 h). The distillate recovered during this first stage in the condenser was collected and analyzed by FTIR. The temperature was then increased to 245°C, the lid was heated at a temperature of 110°C with a heating band, and the reactor was connected to a liquid nitrogen-cooled condenser. Dynamic vacuum was then

Table II. GPC, TGA, and DSC Results of PBS and Its Nanocomposites Synthesized by *In Situ* Polymerization

Samples	$M_w \cdot 10^{-3}$[a]	M_w/M_n[a]	T_{onset} (°C)[b]	T^4_D (°C)[b]	T_{CC} (°C)[c]	ΔH_{CC} (J g^{-1})[c]	T_g (°C)[d]	T_m (°C)[d]	ΔH_m (J g^{-1})[d]
PBSp	54	2.2	373	315	76	72	−34	115	72
PBS-LDH-Cp	43	2.1	346	306	66	62	−34	114	63
PBS-LDH-LSp	53	2.2	362	310	72	61	−37	115	66
PBS-LDH$_{Zn}$-STp	58	2.2	363	325	75	63	−35	113	56
PBS-LDH$_{Mg}$-STp	43	2.2	359	307	70	63	−34	114	66
PBS-LDH-SUp	61	2.6	363	313	65	76	−33	115	81
PBS-LDH-ADp	61	2.6	357	307	65	76	−32	115	86
PBS-LDH-SEp	61	2.3	365	306	67	62	−33	115	71
PBS-LDH-CAp	51	2.5	368	321	68	74	−32	115	77
PBS-LDH-RAp	48	2.2	365	318	65	63	−34	115	67

[a] Determined by GPC in $CHCl_3$.

[b] Determined by TGA at 10°C min^{-1} in N_2.

[c] Determined by DSC during the cooling scan from the melt at 10°C min^{-1}.

[d] Determined by DSC during the second heating scan at 20°C min^{-1}.

applied in 60 min down to 0.1 mbar. After 60 min, a highly viscous, brown, and transparent melt was discharged from the reactor. The molecular structure of PBS was confirmed by ^{1}H-NMR. The new composites are called PBS-LDH-xxp, where LDH-xx is the code of the organo-modified LDH, described in Table I. All the samples are listed in Table II.

Melt Intercalation

PBS–organo-modified LDH nanocomposites were prepared in a Brabender Plasticoder 2000 equipped with an electrically heated mixer. A mixture composed by PBE003 and 3 wt % of the different LDH was introduced in the blender. The internal temperature of the mixer was maintained at 140°C, and the mixing speed was 60 rpm. Blending was activated for 6 min. PBE003m indicates the homopolymer melt blended without the clay.

The new composites are called PBS-LDH-xxm, where LDH-xx is the code of the organo-modified LDH, described in Table I. All the samples are listed in Table III.

Measurements

^{1}H-NMR spectra were recorded on a Varian Mercury 400 spectrometer (chemical shifts are in part per million downfield from TMS); the solvent used was $CDCl_3$.

Gel permeation chromatography (GPC) measurements were performed on a HP 1100 Series using a PL gel 5-μm Mini-mixed-C column with chloroform as eluent and to dissolve polymer samples. A Refractive Index detector was used.

FTIR analysis was conducted over the wave number range of 650–4000 cm^{-1} using a Perkin Elmer Spectrum One FTIR spectrometer equipped with a Universal ATR Sampling Accessory.

Thermogravimetric analysis (TGA) was performed in nitrogen atmosphere using a Perkin-Elmer TGA7 apparatus (gas flow 50 mL min^{-1}) at 10°C min^{-1} heating rate from 40 to 850°C.

The onset degradation temperatures (T_{onset}) were taken from the intersections of the tangents of the initial points and the

Table III. TGA and DSC Results of PBS and Its Nanocomposites Prepared by Melt Intercalation

Samples	T_{onset} (°C)[a]	T^4_D (°C)[a]	T_{CC} (°C)[b]	ΔH_{CC} (J g^{-1})[b]	T_g (°C)[c]	T_m (°C)[c]	ΔH_m (J g^{-1})[c]
PBE003m	372	317	82	66	−29	116	61
PBS-LDH-Cm	362	310	79	67	−32	116	65
PBS-LDH-LSm	365	305	79	63	−33	116	63
PBS-LDH$_{Zn}$-STm	359	314	78	62	−33	115	61
PBS-LDH$_{Mg}$-STm	357	314	76	64	−34	115	62
PBS-LDH-SUm	362	310	78	77	−30	117	84
PBS-LDH-ADm	360	305	77	65	−32	116	65
PBS-LDH-SEm	368	317	78	67	−31	116	71
PBS-LDH-CAm	370	329	80	68	−31	116	65
PBS-LDH-RAm	359	320	72	68	−32	116	71

[a] Determined by TGA at 10°C min^{-1} in N_2.

[b] Determined by DSC during the cooling scan from the melt at 10°C min^{-1}.

[c] Determined by DSC.

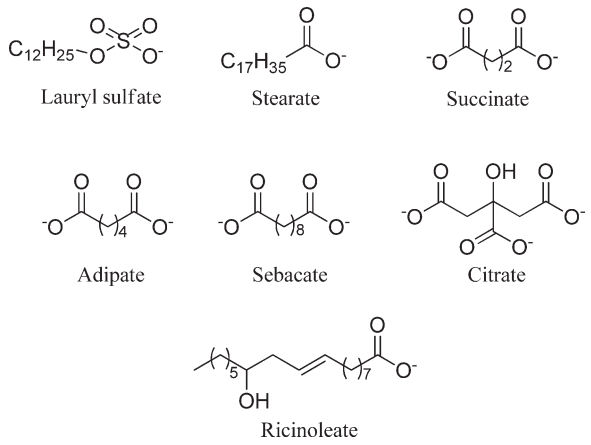

Figure 1. LDHs intercalating anions.

inflection points; the 4% mass loss temperatures (T^4_D) was measured and reported in Tables II and III.

The calorimetric analysis differential scanning calorimetry (DSC) was carried out by means of a Perkin-Elmer DSC6. Measurements were performed under nitrogen flow. To delete their previous thermal history, the samples (~10 mg) were first heated at 20°C min^{-1} to 150°C, kept at high temperature for 5 min, and then cooled to -60°C at 10°C min^{-1}. After this thermal treatment, the samples were analyzed by heating from −60 to 150°C at 20°C min^{-1} (second scan). During the cooling scan, the crystallization temperature (T_{CC}) and the enthalpy of crystallization (ΔH_{CC}) were measured. During the second scan, the glass transition temperature (T_g), the melting temperature (T_m), and the enthalpy of fusion (ΔH_m) were measured. T_g was taken as the midpoint of the heat capacity increment associated with the glass-to-rubber transition.

XRD measurements in steps of 0.07° over 2θ range of 2.2–80° for clay samples and over 2θ range of 2.1–35° for nanocomposite samples, were carried out at room temperature with Bragg/Brentano diffractometers (Philips PW1710 and XPERT-PRO for clay and nanocomposite samples, respectively) with Cu K_α radiation ($\lambda = 0.154$ nm, monochromatization by primary graphite crystal) generated at 40 mA and 40 kV. A flat sample holder, 1.5 mm deep, was filled with sample powder.

The melt rheology properties of the polymer blends were measured at 120°C with a rotational spectrometer (ARES, TA) equipped with a parallel plate geometry (plate diameter 8 mm, gap 1 mm). The imposed oscillatory shear stress amplitude was tested to validate the measurements inside the linear viscoelastic domain. This strain was fixed and used for measuring the dynamic stress against oscillatory shearing frequency (from 0.1 to 100 rad s^{-1}). G' (storage modulus), G'' (loss modulus), and tan δ (ratio of G' and G'') were monitored automatically against frequency. The curve representing the loss viscosity (η'') against elastic viscosity (η') is designed as the Cole–Cole plot.

Physical and mechanical properties were determined using a Rheometric Scientific DMTA IV Dynamic Mechanic Thermo analysis instrument with a dual cantilever testing geometry. Typical test samples were bars obtained by injection molding at 120°C using a Minimix Molder. The analysis was carried out at a frequency of 3 Hz, at 3°C min^{-1} in the temperature range −60 to 80°C.

RESULTS AND DISCUSSION

Preparation of Organo-Modified LDHs

Novel organo-modified anionic clays, whose characteristics are reported in Table I, were prepared and then incorporated into the PBS matrix. Figure 1 shows the organic anions used. It is worth noting that they differ in terms of chemical structure. Lauryl sulfate and stearate possess one charge and a long aliphatic chain; succinate, adipate, and sebacate are short bicarboxylates; citrate and ricinoleate are bearing OH groups that could subsequently react with the functional groups of the polymeric chains.

Figure 2 illustrates the XRD patterns of the organo-modified clays. It comes out that the crystallinity and the structural properties of the LDHs are highly dependent on the nature of the interlayer anions and on the preparation route and conditions.[33] The basal spacing of the LDHs prepared are reported in Table I and were calculated from the peak position (d_{003} reflection) according to the Bragg diffraction law.[34] As can be seen, all the organo-modified clays present the basal peak shifted to lower angles in respect to the LDH containing CO_3^{2-} (LDH-C), characterized by the peak at $2\theta = 11.6°$ ($d = 7.7$ Å). Moreover, CO_2 contamination did not occur during the clay coprecipitation syntheses since the same characteristic peak of the LDH-C is not present in all the other LDHs XRD spectra. In the case of LDH-LS two basal peaks, located at $2\theta = 2.6°$ ($d = 34.4$ Å) and a second one, very weak in relative intensity at $2\theta = 3.6°$ ($d = 24.5$ Å), are present. This suggests that the anion is present in two different orientations, conferring two different layer distances. In any case, the values of the basal spacing of the different LDHs are consistent with the length of the anion molecular chains and with the values reported by other authors.[32,35,36]

The thermal stability of LDHs was checked by TGA analysis which shows that thermal decomposition in all cases occurs in

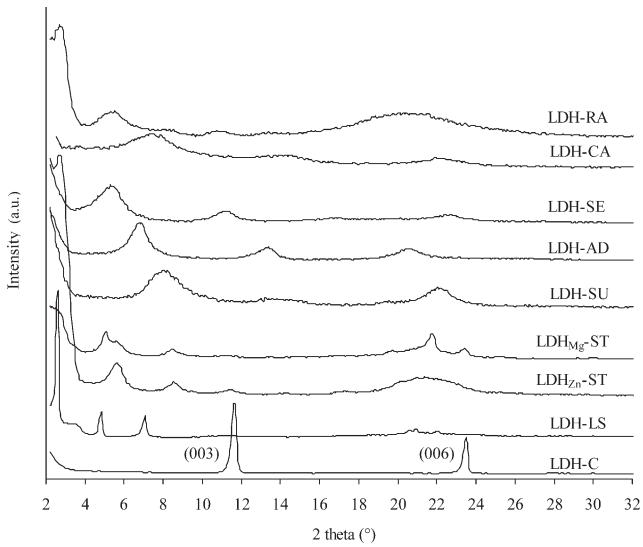

Figure 2. XRD profiles of various LDHs.

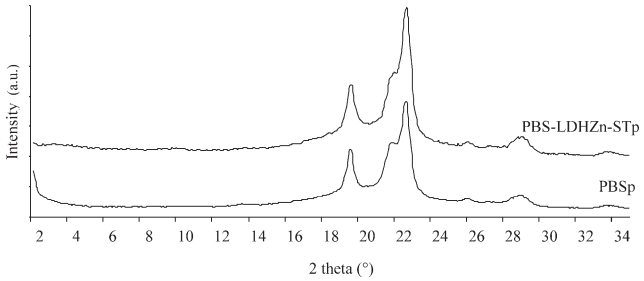

Figure 3. XRD profiles of PBS nanocomposites prepared by *in situ* polymerization.

three stages corresponding to: (I) removal of physisorbed water at the surface and between the hydroxide layers, (II) dehydroxylation of the hydroxide layers, and (III) elimination and combustion of the organic anions leaving residual metal oxides.[37] On the basis of the metal cations charged during the clay syntheses and on the weight loss of TGA stages (I) and (III), the chemical composition of the clays was calculated and the corresponding chemical formula was reported in Table I. As it can be seen, the organic content adequately fits the theoretical stoichiometric amount, with some exceptions: the sample containing Zn shows a poor organic loading; the specimens containing citrate and ricinoleate anions have a high loading of the organic compound and interlayered water. This could be explained considering that both molecules, possessing a carboxyl and a hydroxyl group, can self-react leading to some esterification intermolecular processes of their carboxyl functional groups or through intermolecular hydrogen bonding, thus causing a decrement of the ion charge. Moreover, the coprecipitation reaction for the LDH synthesis with the citrate was carried out with a large excess of the anion.

Preparation of Nanocomposites by *In Situ* Polymerization

All the composites were prepared by using the same amount of organo-modified LDH (3 wt %) following two different procedures: *in situ* polymerization and melt blending.

First, as far as *in situ* polymerization is concerned, the syntheses were carried out according to the method described in ref. 38, where a prestage is used in which diol, modified clay, and catalyst are charged into the reactor to favor the swelling of the clay. All the composites prepared were characterized by GPC analysis and their molecular weight resulted to be high and similar, with a M_w value around 50,000.

The degree of dispersion of the organo-modified LDHs in PBS matrix was evaluated by XRD analysis. In Figure 3, as the same results were obtained for all the samples, only a representative PBS-LDH composite was reported, showing the diffraction lines characteristic of PBS and the absence of the diffraction lines of the filler, suggesting that an exfoliation process had probably occurred.

Figure 4 reports TGA thermograms for some representative PBS-LDHp samples, while Table II lists all the results from TGA and DSC analyses of the nanocomposites obtained by *in situ* polymerization. Figure 4 shows a main decomposition process for all the samples in the range 360–375°C. It is notable that the nanocomposites are characterized by T_{onset}, that is always located at lower temperatures than that of PBSp. Accordingly, the temperatures at which the nanocomposites lose a determined amount of weight (e.g., 4%, at T^4_D) are generally lower than that of PBS, with a small number of exceptions, that is, in the presence of LDH containing Zn, LDH-CA, and LDH-RA. Therefore, it is possible to state that for most composites the incorporation of LDH does not improve their thermal stability. Similar phenomena were reported for the same systems[28] and also for PCL/LDH,[39] PPC/LDH,[40] and PLLA/LDH.[41] The reduction of T_{onset} may be attributed to the presence of Mg and Al metals in PBS matrix that can catalyze the intermolecular and intramolecular transesterifications of the polyesters.[42]

In addition, it is also reported that, in the case of polyamides, LDH can decrease the thermal stability of polymer due to accelerated chain hydrolysis arising from water released from the decomposed LDH.[43] On the other hand, the LDH containing Zn performs best, confirming that this metal slows down the hydrolitic processes occurring during the heating.[30,31] Moreover, the relatively high thermal stability of the composites containing LDH-CA and LDH-RA can be ascribed to the possibility that CA and RA groups, which exceed the theoretical composition of LDH, are physisorbed in the inorganic lamellae giving rise to polycondensation reactions with the monomers. This process could determine the formation of crosslinked or modified chemical structures into the original matrix, leading to a higher thermal stability.

The modifications occurring in the polymeric matrix were checked by ^{1}H-NMR, which confirmed the presence of CA and reacted and unreacted RA (figure available as online Supporting Information).

In any case, the degradation temperatures, in particular T^4_D, are consistently higher than the melting temperatures of PBS and the relative composites (see DSC data): therefore, it is quite possible that polymer processing can occur without degradation problems.

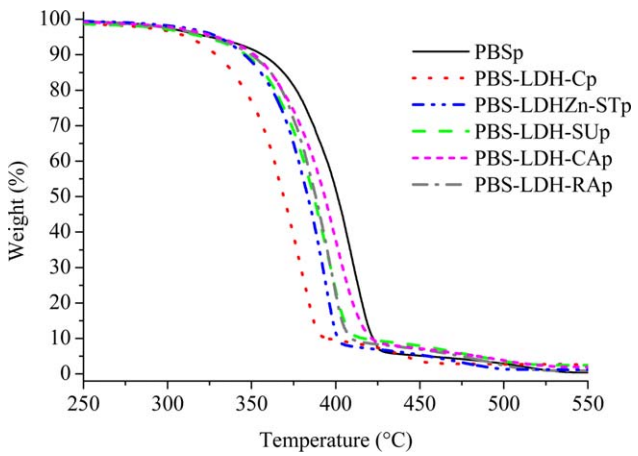

Figure 4. TGA thermograms of PBS nanocomposites prepared by *in situ* polymerization. [Color figure can be viewed in the online issue, which is available at wileyonlinelibrary.com.]

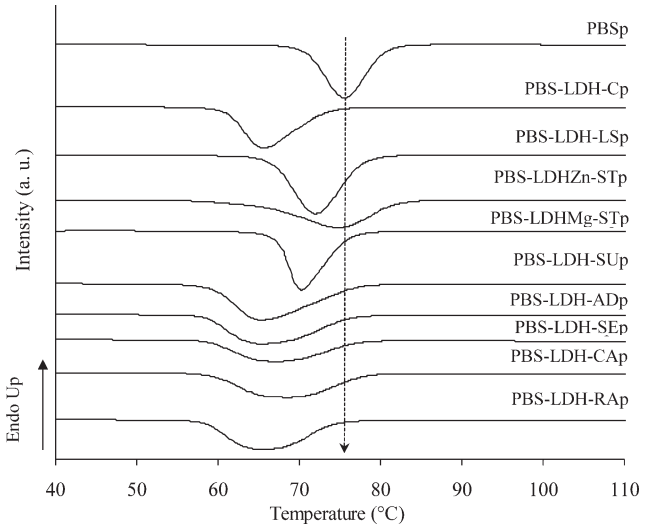

Figure 5. T_{CC} profiles obtained by DSC during the cooling scan for PBS-LDHs prepared by *in situ* polymerization.

From the results of the DSC analysis, reported in Table II, it can be noted that T_m values of the nanocomposites remain fairly constant at around 115°C, independent of the chemical nature of the LDHs. Moreover the peak shapes are always multiple and complex, very similar to that of the pristine PBS. Therefore, the presence of an exfoliated structure does not modify the crystalline phase of PBS, as confirmed by XRD analysis. However, from ΔH_{cc} data, which can be easily measured, it is notable that the PBS-LDH-SUp and PBS-LDH-ADp samples are characterized by a slightly higher degree of crystallinity, ascribable to the fact that the LDH anion, in the first case, is the same comonomer of PBS and obviously adipate unit is quite similar; thus, the chemical formulation remains more homogeneous leading to an easier packing of the macromolecular chains.

On the other hand, the T_{CC} values of Table II indicate that the crystallization rates of PBS-LDH samples are slower than that of PBS homopolymer. From the crystallization process, shown in Figure 5, it is possible to state that the composites tend to crystallize with more difficulty. Such behavior might stem from the fact that the movements of the polymer chains in the melt are restricted by the clay platelets which act as obstacles for the mobility of the chains to join the crystallization growth front. This behavior confirms a good degree of homogeneous dispersion of the LDHs in the PBS matrix.

Considering the T_g values (Table II), in general nanofillers influence the T_g of polymer matrices by two contradictory effects:[44] reduction of the chain mobility and increment of the free volume due to the presence of the rigid nanosheets. The former tends to increase the T_g values while the latter tends to decrease them. In Table II, the T_g values are fairly constant indicating that probably both contributions are present and counterbalanced.

To characterize the microstructural change of the composites prepared, rheology in the melt state was investigated (Figure 6). From the Cole–Cole formalism, most of the composites prepared by *in situ* polymerization method present a higher viscosity as compared to PBS homopolymer. The only sample featuring a lower viscosity is the one containing citrate as intercalating LDH ions. This means that the incorporation of LDH-CA into PBS is not improving the mechanical properties of the polymer probably because of the excess of CA physisorbed in the lamellae. Moreover, the Cole–Cole representation suggests a finite molecular weight for some of the samples, PBS-LDH-CAp, PBS-LDH-SEp, PBS-LDH-RAp, PBS-LDH-SUp, PBS-LDH$_{Mg}$-ST, and PBS-LDH-Cp since a finite value can be extrapolated from the convex downward semicircle at the intercept $\eta'' \rightarrow 0$ which corresponds to the Newtonian zero-shear viscosity η_0 at $\omega = 0$ and is associated to an apparent molecular weight.

In contrast, in the case of PBS-LDH$_{Zn}$-STp and PBS-LDH-LSp, the semiarc becomes a straight line showing the presence of a gel-like PBS structure with no apparent finite molecular weight, indicating a PBS nanocomposite structure.[26,45] In any case the LDH samples showing the greater reinforcing effect are PBS-LDH$_{Zn}$-STp > PBS-LDH-Cp > PBS-LDH$_{Mg}$-STp > PBS-LDH-

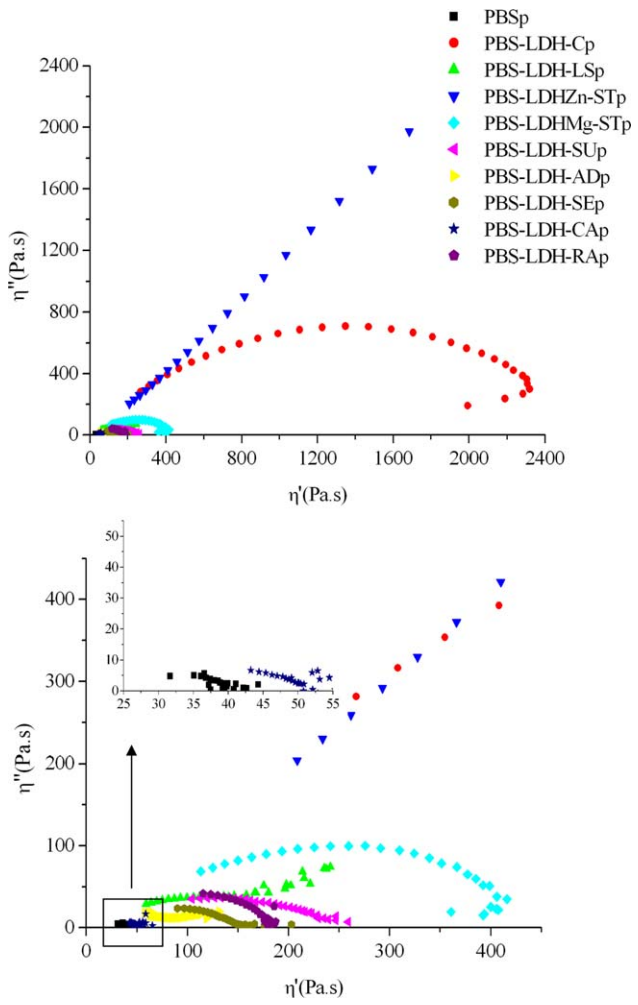

Figure 6. Cole-Cole η''-η' (ω) of PBS-LDHp prepared by *in situ* polymerization. [Color figure can be viewed in the online issue, which is available at wileyonlinelibrary.com.]

Applied Polymer SCIENCE

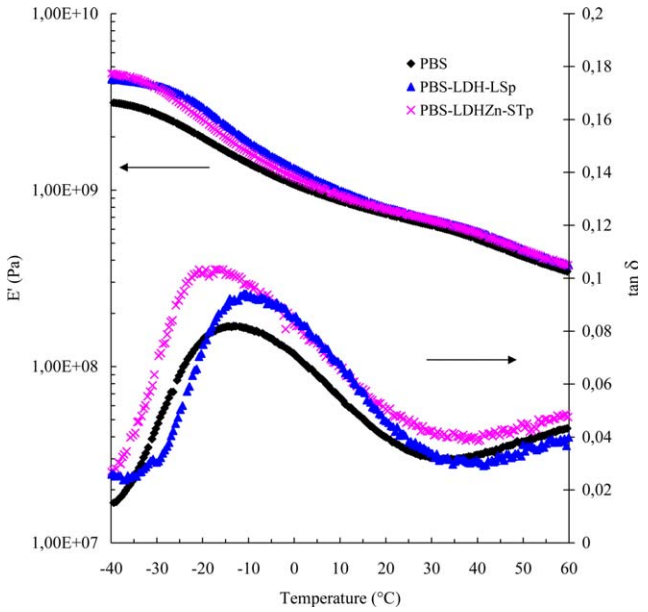

Figure 7. DMTA spectra for PBS-LDHp prepared by *in situ* polymerization. Storage modulus (E') and tan δ as a function of temperature. [Color figure can be viewed in the online issue, which is available at wileyonlinelibrary.com.]

LSp > PBS-LDH-SUp > PBS-LDH-RAp > PBS-LDH-SEp > PBS-LDH-ADp. Therefore, apart from the sample containing the carbonate ion, the reinforcing effects are in the order of the interlayer LDH dimensions, that is, to say that a higher anion size corresponds to a higher reinforcing effect, probably caused by a better dispersability and exfoliation as well as by a more efficient friction between tethered surfactant-based molecules and PBS chains. In the case of ricinoleate, the anion dimension is probably compensated with the plasticizing effect of the anion physisorbed on the LDH lamellae. Regarding the LDH samples containing the bicarboxylate ions, the succinate anion, although the smallest one, grants a much higher enhancement of the reinforcing effect, probably given its molecular affinity with the polymer molecular chain.

Dynamic mechanical properties of PBS-LDH samples were also investigated. Figure 7 shows the dynamic storage modulus (E') as a function of temperature for PBS and PBS nanocomposites containing LDH-LS and LDH_{Zn}-ST. As can be seen, the values of E′ are higher for the nanocomposites, giving rise to a reinforcing effect of the PBS matrix and confirming the results obtained with the melt rheological properties. In the case of the other nanocomposites, which were not reported in the figure, no significant differences were observed in respect to the homopolymer. Furthermore, glass transition temperature can be extrapolated considering the tan δ maximum peak visible in Figure 7. The homopolymer exhibits a T_g of −15°C, while the sample with lauryl sulfate modified LDH presents a value of −10°C and PBS-LDH_{Zn}-ST shows a T_g of −20°C: these differences which do not result from DSC analyses, should probably be ascribed to the different intrinsic sensitivities between both related techniques. In general, DMTA, where T_g is frequency dependent and increases with increasing frequency, is a more sensitive technique than DSC where T_g depends on the heating rate.[46] Data obtained supports the above hypothesis regarding the presence of two contributions: in case of PBS-LDH-LSp reduction of the chain mobility prevails, while in the nanocomposite containing LDH_{Zn}-ST, the free volume due to the presence of the rigid nanosheets, predominates.

Therefore, LDH nanosheets, modified with anions of large dimensions, resulted delaminated in PBS matrix leading to improved mechanical performances. This interesting result is obtained by preparing the bionanocomposites by direct polymerization from monomers.

Preparation of Nanocomposites by Melt Blending

Regarding the samples prepared by melt blending, the X-ray analysis (Figure 8) shows that only some of the composites prepared present a fully exfoliated structure: PBS-LDH-LSm, PBS-LDH_{Zn}-STm, PBS-LDH_{Mg}-STm, PBS-LDH-CAm, and PBS-LDH-RAm. The samples with carbonate, succinate, adipate, and sebacate anions as intercalating LDH molecules present the identical first diffraction line of the starting organo-modified LDH, suggesting that the interlamellae space is unchanged and, in this case, only a partial intercalation process occurred, probably caused by the low interlayer LDH distance.

Accordingly, a minor effect on the crystallization rate, Table III and Figure 9, is obvious apart from the nanocomposites with ricinoleate, which present the lowest T_{CC} value confirming a good dispersion of the clay and/or, being the ricinoleate anion in excess, the reaction of this monomer itself, confirmed by ^{1}H-NMR analysis.

It is notable that with the melt blending nanocomposites preparation technique as well, T_m values remain constant but with PBS-LDH-SUm sample characterized by a slightly higher degree of crystallization only.

Considering the T_g values (Table III), as stated in the previous paragraph, generally nanofillers influence the T_g of polymer matrices by two contradictory effects:[44] reduction of the chain mobility and increment of the free volume. In Table III, it

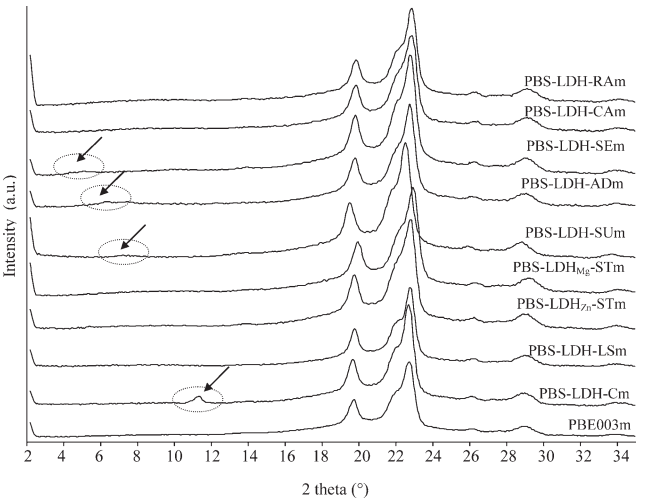

Figure 8. XRD profiles of PBS nanocomposites prepared by melt blending.

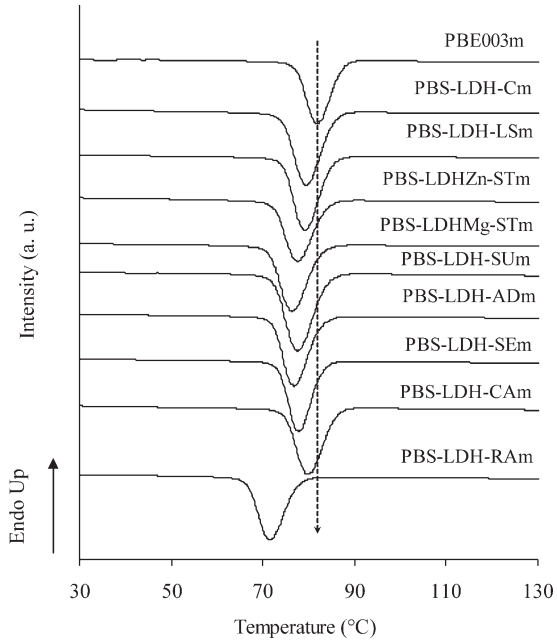

Figure 9. T_{CC} profiles obtained by DSC during the cooling scan for PBS-LDHs prepared by melt intercalation.

appears that the effect of the increased free volume dominates, leading to a slight decrease in the T_g.

Regarding the TGA data (Table III), the same trends as the case of the *in situ* polymerization technique may be considered, since the range of thermal decomposition is the same but in this case, the effect of Zn, as metal cation, is less pronounced.

In Figure 10, the Cole–Cole representation for the composite samples prepared by melt blending, suggests that the reinforcing effect of the organo-modified LDHs is lower with respect to the same samples prepared by the *in situ* polymerization method and no gel-like structure is observed. In any case, the viscosity

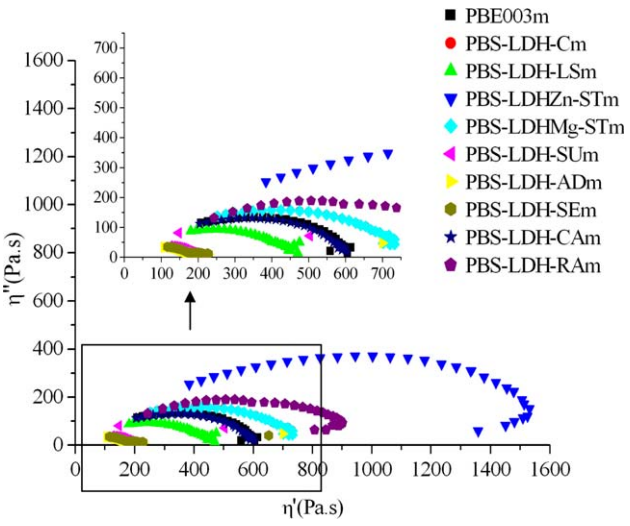

Figure 10. Cole–Cole η''-η' (ω) of PBS-LDHm prepared by melt blending. [Color figure can be viewed in the online issue, which is available at wileyonlinelibrary.com.]

increment is in the following order: PBS-LDH$_{Zn}$-STm > PBS-LDH-RAm > PBS-LDH$_{Mg}$-STm = PBS-LDH-Cm. The samples PBS-LDH-LSm, PBS-LDH-CAm and those prepared with the carboxylate anions have no effect in reinforcing the PBS matrix, indicating again that the dimension of the interlayer region of LDH plays an important role in developing a large interface between the filler and the polymer.

Moreover, no enhancement in the dynamic mechanical properties was achieved (data not shown): all samples tested highlighted poor differences in respect to the homopolymer. Therefore, the melt blending procedure shows a poor capability in inducing delamination in the nanocomposites.

CONCLUSIONS

In this work, PBS-LDH composites were prepared by *in situ* polymerization and melt blending. To enhance the compatibility between PBS and LDH several aliphatic organic anions were successfully intercalated in the lamellar structure by the conventional coprecipitation method. The techniques used for the dispersion of the clay in the PBS matrix as well as the dimension of the organic interlamellar layer have been shown to play a significant role in determining an improvement of the melt rheological properties and dynamic mechanical properties. In particular, the *in situ* polymerization method demonstrated to be more effective for the production of the nanocomposite structures, probably due to a longer-lasting mixing with the PBS monomers. The stearate ions, dispersed in the LDH structure, gave rise to the nanocomposite with the best thermal and mechanical performance, in particular the one prepared with zinc as metal cation, which produced a gel-like structure. Among the other intercalating ions, the succinate, being also a comonomer for PBS, showed that a more homogeneous material can be achieved resulting in a more crystalline final polymer material.

In conclusion, this work presents significant added values:

1. the use of renewable organic molecules to modify fillers;
2. the identification of the stearate ion, as the best modifier;
3. the preparation of new nanocomposites which are potentially fully biodegradable.

Stearic acid is frequently used as polymer industrial stabilizer[47] and is not costly. Thus, it is possible in the future to set-up a new formulation for sustainable different applications, for example, for food packaging, and gas barrier properties are under investigation.

REFERENCES

1. Li, H.; Chang, J.; Cao, A.; Wang, J. *Macromol. Biosci.* **2005**, *5*, 433.
2. Xu, J.; Guo, B. H. *Biotechnol. J.* **2010**, *5*, 1149.
3. Fujimaki, T. *Polym. Degrad. Stab.* **1998**, *59*, 209.
4. Han, S. I.; Lim, J. S.; Kim, D. K.; Kim, M. N.; Im, S. S. *Polym. Degrad. Stab.* **2008**, *93*, 889.

5. Vassiliou, A. A.; Bikiaris, D.; El Mabrouk, K. *J. Appl. Polym. Sci.* **2011**, *119*, 2010.
6. Bian, J.; Han, L.; Wang, X. *J. Appl. Polym. Sci.* **2010**, *116*, 902.
7. Zhou, W.; Xu, T.; Wang, X.; Zhi, E.; Liu, J.; Zhang, W.; Ji, J. *J. Appl. Polym. Sci.* **2013**, *127*, 733.
8. Tan, L.; Che, Y.; Zhou, W.; Ye, S.; Wei, J. *Polymer* **2011**, *52*, 3587.
9. Hong, M. K.; Ko, S. W.; Park, J. H.; Choi, H. J.; Kim, J. H. *J. Nanosci. Nanotechnol.* **2011**, *11*, 5352.
10. Pramoda, K. P.; Linh, N. T. T.; Zhang, C. *J. Appl. Polym. Sci.* **2009**, *111*, 2938.
11. Wang, X. W.; Zhang, C. A.; Wang, P. L.; Zhao, J.; Zhang, W.; Ji, J. H.; Hua, K.; Zhou, J.; Yang, X. B.; Li, X. P. *Langmuir* **2012**, *28*, 7091.
12. Phua, Y. J.; Chow, W. S.; Ishak, Z. A. M. *J. Thermoplast. Compos. Mater.* **2011**, *24*, 133.
13. Shih, Y. F.; Wang, T. Y.; Jeng, R. J.; Wu, J. Y.; Teng, C. C. *J. Polym. Environ.* **2007**, *15*, 151.
14. Someya, Y.; Nakazato, T.; Teramoto, N.; Shibata, M. *J. Appl. Polym. Sci.* **2004**, *91*, 1463.
15. Zhan, M. Q.; Chen, G. Y.; Wei, Z. Y.; Shi, Y. M.; Zhang, W. X. *Chin. J. Polym. Sci.* **2013**, *31*, 187.
16. Costantino, U.; Nocchetti, M.; Tammaro, L.; Vittoria, V. *Recent Pat. Nanotechnol.* **2012**, *6*, 218.
17. Oh, J. M.; Choi, S. J.; Lee, G. E.; Kim, J. E.; Choy, J. H. *Chem. Asian J.* **2009**, *4*, 67.
18. Oh, J. M.; Park, D. H.; Choi, S. J.; Choy, J. H. *Recent Pat. Nanotechnol.* **2012**, *6*, 200.
19. Kafunkova, E.; Lang, K.; Kubat, P.; Klementova, M.; Mosinger, J.; Slouf, M.; Troutier-Thuilliez, A.-L.; Leroux, F.; Verney, V.; Taviot-Gueho, C. *J. Mater. Chem.* **2010**, *20*, 9423.
20. Utraki, L. A.; Sepehr, M.; Boccaleri, M. *Polym. Adv. Technol.* **2007**, *18*, 1.
21. Cavani, F.; Trifirò, F.; Vaccari, A. *Catal. Today* **1991**, *11*, 173.
22. Zou, H.; Wu, S.; Shen, J. *Chem. Rev.* **2008**, *108*, 3893.
23. Yang, F.; Nelson, G. L. J. *Appl. Polym. Sci.* **2004**, *91*, 3844.
24. Hwang, S. S.; Liu, S P.; Hsu, P. P.; Yeh, J. M.; Yang, J. P.; Chang, K. C.; Chu, S. N. *Int. Commun. Heat Mass.* **2011**, *38*, 1219.
25. Hernández, J. J.; García-Gutiérrez, M. C.; Nogales, A.; Rueda, D. R.; Kwiatkowska, M.; Szymczyk, A.; Roslaniec, Z.; Concheso, A.; Guinea, I.; Ezquerra, T. A. *Compos. Sci. Technol.* **2009**, *69*, 1867.
26. Zhou, Q.; Verney, V.; Commereuc, S.; Chin, I. J.; Leroux, F. *J. Colloid Interface Sci.* **2010**, *349*, 127.
27. Okamoto, K.; Ray, S. S.; Okamoto, M. *J. Polym. Sci. Polym. Phys.* **2003**, *41*, 3160.
28. Wei, Z.; Chen, G.; Shi, Y.; Song, P.; Zhan, M.; Zhang, W. *J. Polym. Res* .**2012**, *19*, 9930.
29. Lim, J. S.; Hong, S. M.; Kim, D. K.; Im, S. S. *J. Appl. Polym. Sci.* **2008**, *107*, 3598.
30. Costantino, U.; Gallipoli, A.; Nocchetti, M.; Camino, G.; Bellucci, F.; Frache, A. *Polym. Degrad. Stab.* **2005**, *90*, 586.
31. Manzi-Nshuti, C.; Wang, D.; Hossenlopp, J. M.; Wilkie, C. A. *J. Mater. Chem.* **2008**, *18*, 3091.
32. Zhang, J.; Zhang, F.; Ren, L.; Evans, D. G.; Duan, X. *Mater. Chem. Phys.* **2004**, *85*, 207.
33. Costantino, U.; Marmottini, F.; Nocchetti, M.; Vivani, R. *Eur. J. Inorg. Chem.* **1998**, *1*, 1439.
34. Zachariasen, W. H. Theory of X-Ray Diffraction in Crystals. Dover Publications: New York, **1994**.
35. Drezdzon, M. A. *Inorg. Chem.* **1988**, *27*, 4628.
36. Iyi, N.; Tamura, K.; Yamada, H. *J. Colloid Interface Sci.* **2009**, *340*, 67.
37. Zhu, L.; Su, S.; Hossenloop, J. M. *Polym. Adv. Technol.* **2012**, *23*, 171.
38. Berti, C.; Fiorini, M.; Sisti, L. *Eur. Polym. J.* **2009**, *45*, 70.
39. Costantino, U.; Bugatti, V.; Gorrasi, G.; Montanari, F.; Nocchetti, M.; Tammaro, L.; Vittoria, V. *ACS Appl. Mater. Interfaces* **2009**, *1*, 668.
40. Du, L. C.; Qu, B. J.; Meng, Y. Z.; Zhu, Q. *Compos. Sci. Technol.* **2006**, *66*, 913.
41. Eili, M.; Shameli, K.; Ibrahim, N. A.; Yunus, W. M. Z. W. *Int. J. Mol. Sci.* **2012**, *13*, 7938.
42. Chiang, M. F.; Chu, M. Z.; Wu, T. M. *Polym. Degrad. Stab.* **2011**, *96*, 60.
43. Herrero, M.; Benito, P.; Labajos, F. M.; Rives, V.; Zhu, Y. D.; Allen, G. C.; Adams, J. M. *J. Solid State Chem.* **2010**, *183*, 1645.
44. Rotrekl, J.; Matějka, L.; Kaprálková, L.; Zhigunov, A.; Hromádková, J.; Kelnar, I. *Express Polym. Lett.* **2012**, *6*, 975.
45. Xu, L.; Nakajima, H.; Manias, E.; Krishnamoorti, R. *Macromolecules* **2009**, *42*, 3795.
46. Foreman, J.; Sauerbrunn, S. R.; Marcozzi, C. L. Exploring the Sensitivity of Thermal Analysis Techniques to the Glass Transition; TA Instruments: New Castle, DE. Available at: http://www.tainstruments.co.jp/application/pdf/Thermal_Library/Applications_Briefs/TA082.PDF. Accessed on 10 April 2013.
47. Zweifel, H. In Plastics Additives Handbook, 5th ed.; Zweifel, H., Ed.; Hanser: Munich, **2001**; Chapter 17, p 934.